STUDIES TO IMPROVE THE PERFORMANCE OF CHEMICALLY MODIFIED ELECTRODES BASED ON E-5-((5-ISOPROPYL-3,8-DIMETHYLAZULEN-1-YL)DIAZENYL)--1H-TETRAZOLE FOR HEAVY METAL IONS ANALYSIS

Adina-Maria PĂUN[1], Ovidiu-Teodor MATICA[2], Laura-Bianca ENACHE[3], Elena DIACU[4], Eleonora-Mihaela UNGUREANU*[5], Marius ENACHESCU[6]

*E-5-((5-isopropyl-3,8-dimethylazulen-1-yl)diazenyl)-1H-tetrazole (**L**) was used to obtain chemically modified electrodes (CMEs) based on **L** (**L**-CMEs) for heavy metals (HMs) analysis in water. The studies were performed by: chronoamperometry and cyclic voltammetry. To optimize the preparation conditions of CMEs, **L** films were deposited by controlled potential electrolysis at various anodic charges and potentials. **L**-CMEs were tested for HMs ions analysis from mixed solutions of Cd(II), Pb(II), Cu(II), and Hg(II). Those that showed the best analytical signals were examined by scanning electron microscopy and atomic force microscopy to show the influence of the preparation conditions of CMEs on the characteristics of films.*

Keywords: E-5-((5-isopropyl-3,8-dimethylazulen-1-yl)diazenyl)-1H-tetrazole, voltammetric techniques, chemically modified electrodes, scanning electron microscopy, atomic force microscopy

1. Introduction

Heavy metals and metalloids such as Cd(II), Pb(II), Hg(II), As(III), As(V) are a major threat to living organisms due to their tendency to accumulate and their slow speed of release in the body. This alters metabolic functions leading to dysfunction of vital organs and glands (e.g., heart, liver, kidneys, brain, bones, etc.) [1]. The toxicity of the Cd(II), Pb(II) and Hg(II) ions on the human body relates to the chemical form, the quantity, and the level of exposure [2, 3]. The

[1] Ph D student, Dept. of Analytical Chemistry, and Environmental Engineering, University POLITEHNICA of Bucharest, Romania, e-mail: paunadina4@gmail.com
[2] Ph D student, Dept. of Inorganic Chemistry, Physical Chemistry and Electrochemistry, University POLITEHNICA of Bucharest, Romania, e-mail: maticaovidiu@yahoo.co.uk
[3] Ph D student, Dept. of Inorganic Chemistry, Physical Chemistry and Electrochemistry, University POLITEHNICA of Bucharest, Romania, e-mail: laurabianca2794@gmail.com
[4] Emeritus Professor, Dept. of Analytical Chemistry, and Environmental Engineering, University POLITEHNICA of Bucharest, e-mail: elena_diacu@yahoo.co.uk
*[5]Emeritus Professor, Dept. of Inorganic Chemistry, Physical Chemistry and Electrochemistry, University POLITEHNICA of Bucharest, e-mail: em_ungureanu2000@yahoo.com
[6] Professor, Center for Surface Science and Nanotechnology, University POLITEHNICA of Bucharest, Romania: e-mail: marius.enachescu@cssnt-upb.ro

increase of heavy metal concentrations is mainly due to anthropogenic activities and not necessarily because of their natural presence in the environment. Therefore, the detection and monitoring of these elements in contaminated environments (water, air, and soil) require efficient and less expensive techniques.

Currently, classical techniques such as atomic absorption, emission, fluorescence or mass spectrometry [4] have alternatives such as UV-Vis spectroscopy, fluorescence spectroscopy or voltammetric stripping techniques that allow a quick and easy detection of metal ions. The voltammetric stripping techniques based on modified electrodes are a promising alternative leading to a portable method at lower cost than the classical techniques. The use of complexing chemical modified electrodes ensures an increase in the selectivity and sensitivity of the analysis. These complexing CMEs can be obtained by coating the electrodes with complexing polymer films. The most efficient method of preparing the latter is the direct electropolymerization of a complexing monomer [5]. E-5-((5-isopropyl-3,8-dimethylazulen-1-yl)diazenyl)-1H-tetrazole (**L**) is an azulene monomer (Fig. 1) which was previously described [6] and characterized by electrochemical techniques [7], which has been shown to be a good complexant for heavy metal ions especially for Pb(II). Azulenes are bicyclical aromatic compounds with a polar structure containing a cyclopentadienyl anion fused to a cycloheptatrienylium cation [8]. Due to their structure, with charges separated on the two cycles, azulene derivatives have electrochemical properties that allow their polymerization [9].

This paper shows several studies carried out to improve the performance of HMs detection using chemically modified electrodes (CMEs) based on **L** (denoted **L**-CMEs). **L**-CMEs were obtained in various conditions and tested for HMs analysis in water solutions. Those that showed the best analytical signals were examined by surface studies using scanning electron microscopy (SEM) and atomic force microscopy (AFM) to show the influence of the preparation conditions on the characteristics of films.

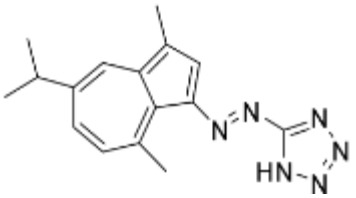

Fig.1. Structure of the ligand used to obtain the chemically modified electrodes

2. Experimental

Reagents

The ligand **L** was synthesized according to the previously published procedure [6, 7]. For the electrochemical experiments an organic electrolyte tetrabutylammonium perchlorate (TBAP) dissolved in acetonitrile (CH_3CN) as solvent were used. The modified electrodes were conditioned in 0.1 M acetate

buffer (pH = 4.5), prepared from solutions of 0.2 M acetic acid, 0.2 M sodium acetate and ultrapure water. Solutions of various concentration of HMs salts used in chemical preconcentration were prepared before each experiment from the 10^{-3} M stock solutions of the following salts: mercury(II) acetate, cadmium(II) acetate dihydrate, lead(II) acetate trihydrate and copper(II) acetate monohydrate.

Apparatus

The electrochemical experiments were performed in standard electrochemical cells connected to AUTOLAB 302N potentiostat. The working electrode was a glassy carbon (GC) disk (d = 3 mm, Metrohm). Three electrochemical cells were used to obtain and characterize the polymeric films deposited on the glassy carbon electrode, namely, the synthesis cell *SC* and two transfer cells. The transfer cell *TC1*, containing either the supporting electrolyte (0.1 M TBAP/ CH_3CN) or 1 mM solution of ferrocene in the supporting electrolyte was used to characterize the CMEs in organic medium, and the transfer cell *TC2* containing 0.1 M acetate buffer (pH = 4.5) was used for conditioning (by equilibration and overoxidation), and for the stripping step during HMs analysis. The reference electrodes used were Ag/10 mM AgNO3, 0.1 M TBAP/ CH3CN (for experiments in organic medium) and Ag/AgCl, 3 M KCl (for experiments in aqueous medium). The auxiliary electrodes were Pt wires.

The samples analysed by scanning electron microscopy (SEM) and atomic force microscopy (AFM) were obtained on bigger GC disks (d = 6 mm) which were electrochemically modified with **L** in solutions of **L** (1 mM in 0.1 M TBAP/ CH_3CN).

A Hitachi SU 8230 system was used for the SEM studies, the samples being analysed at a low acceleration voltage (5 to 10 kV) to prevent damage. The properties of the **L**-CMEs surfaces were analysed by AFM using a multimodal NTEGRA System atomic force microscope, NT-MDT. The AFM measurements were carried out using a HA_HR/50 cantilever with the spring constant of 17 N/m and 230 kHz resonance frequency.

Procedures

The chemically modified electrodes with **L** (**L**-CMEs) were prepared in *SC* in solutions of **L** (1 mM) in 0.1 M TBAP/ CH_3CN by controlled potential electrolysis (CPE) or by scanning in the domain of anodic potentials using cyclic voltammetry (CV). **L**-CMEs characterization by ferrocene probe was performed in *TC1* in millimolar ferrocene solutions in 0.1 M TBAP/ CH3CN by cyclic voltammetry (CV). **L**-CMEs conditioning was performed in *TC2* containing 0.1 M acetate buffer (pH = 4.5) and consisted of 15 CV equilibration cycles (at 0.1 V/s between - 0.9 V and + 0.6 V), and 15 CV overoxidation cycles (at 0.1 V/s between - 0.2 V and + 1.5 V).

For HMs analysis experiments the modified electrodes prepared by CPE in *SC* were cleaned in acetonitrile, conditioned in acetate buffer solution in *TC1*, and immersed in accumulation solutions containing heavy metal ions (Cd(II), Pb(II), Hg(II) and Cu(II)) at different concentrations of all cations, under magnetic

stirring for 15 minutes. After this chemical preconcentration, **L**-CMEs complexed with metal ions were rinsed with distilled water, introduced into the analysis cell (*TC2*) containing 0.1 M acetate buffer solution (pH 4.5), and the potential of -1 V was applied for 3 minutes. Then the DPV curves were recorded between -1 V and +0.6 V. The test solutions of HMs used in chemical preconcentration (with concentrations between 10^{-4} and 10^{-9} M) were freshly prepared in ultrapure water. The CV curves were recorded at scan rates of 0.1 V/s and 0.05 V/s, and the DPV curves were obtained at 0.01 V/s, with a pulse height of 0.025 V and a time interval of 0.2 s. The DPV currents for each metal were measured by subtracting the background from the present current. The potentials were referred when necessary to the potential of the reversible ferrocene/ ferricinium system (Fc/ Fc^+). For the samples analysed by AFM the measurements were done on an area of 10x10 μm^2, where height (topography) and phase signals were acquired simultaneously.

3. Results and Discussion

Table 1 shows the investigated samples of **L**-CMEs obtained by CPE at different charge densities and potentials in solution of **L** (1mM) in 0.1 M TBAP/ CH_3CN. The samples prepared on standard GC disks (d = 3 mm) are denoted CME (CME1-CME11), and those on pellet form (d = 6 mm) electrodes are denoted CMEp (CME12p - CME19p). The samples on standard GC disks were examined by chronoamperometry during their formation by CPE and tested by CV in 0.1M TBAP/ CH_3CN or in ferrocene solution in 0.1M TBAP/ CH_3CN and used for HMs' analysis (CME1 - CME11). The samples on GC pellets were examined by chronoamperometry during the formation and tested by CV in ferrocene solution in 0.1M TBAP/ CH_3CN or used to examine the surface characteristics by SEM and AFM.

Chronoamperograms during L-CMEs preparation

Fig. 2**A** and Fig. 3**A** show the chronoamperograms recorded on GC pellets (6 mm) at different potentials (0.5 V, 0.8 V, 1V, 1.5 V and 2.5 V) for constant charges of 8 mC (Fig. 2A) and 4 mC (Fig. 3**A**).

During the preparation of all **L**-CMEs samples the chronoamperograms were recorded (Fig. 2 - 5) to check the charge and the reproducibility of films formation.

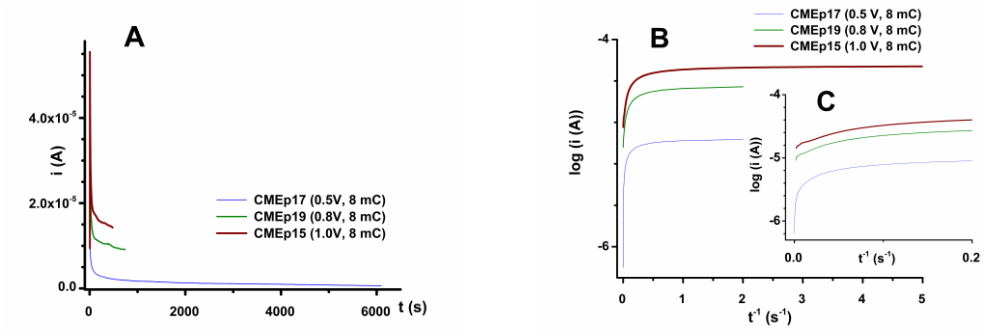

Fig. 2. Chronoamperograms recorded on GC pellets (6 mm in diameter) in different coordinates: i - t (A), logi - t-1 (B, C); the films were obtained by CPE using the same charge of 8 mC and different potentials: 0.5 V (CMEp17), 0.8 V (CMEp19), 1 V (CMEp15)

Table 1

Preparation conditions and tests of L-CMEs on GC disks with diameters of 3 mm (denoted CME) or 6 mm (denoted CMEp)

Sample	CPE potential (V)	CPE charge (mC)	CPE charge density (mC/cm^2)	Tests*
CME1a	1	0.5	7.04	HMs
CME1b	1	1	14.08	Fc, HMs
CME1c	1.25	1	14.08	TBAP
CME1	1	2	28.16	Fc
CME2	1	3	42.25	Fc
CME3	1	4	56.33	Fc
CME3b	1	6	84.48	Fc, HMs
CME4	0.5	0.5	7.04	HMs
CME5	0.5	1.79	25.21	-
CME6	0.5	1.74	24.52	HMs
CME7	0.5	2	28.16	Fc
CME8	0.8	2	28.16	Fc
CME9	0.5	2	28.16	HMs
CME10	0.5	2	28.16	HMs
CME11	0.5	1	14.08	HMs
CMEp12	2.5	4	14.08	SEM
CMEp13	1.5	4	14.08	SEM
CMEp14	1	4	14.08	SEM
CMEp15	1	8	28.16	SEM
CMEp16	1	24	84.48	SEM
CMEp17	0.5	8	28.16	SEM, AFM
CMEp18	0.5	7.4	26.05	SEM, AFM
CMEp19	0.8	8	28.16	SEM

* Type of investigation: HMs (analysis); Fc (ferrocene redox probe); TBAP (CV in 0.1 M TBAP/ CH_3CN), SEM; AFM

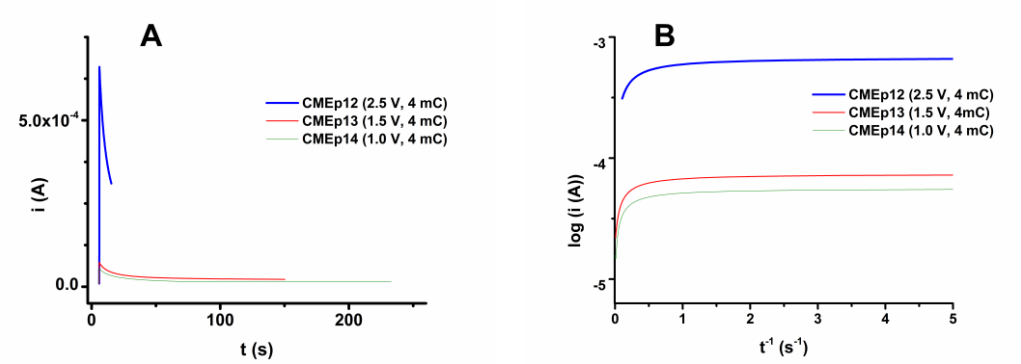

Fig. 3. Chronoamperograms recorded on GC pellets (6 mm in diameter) in different coordinates: *i* - *t* (**A**), *logi* - t^{-1} (B); the films were obtained by CPE using the same charge of 4 mC and different potentials: 1 V (CMEp14), 1.5 V (CMEp13), 2.5 V (CMEp12)

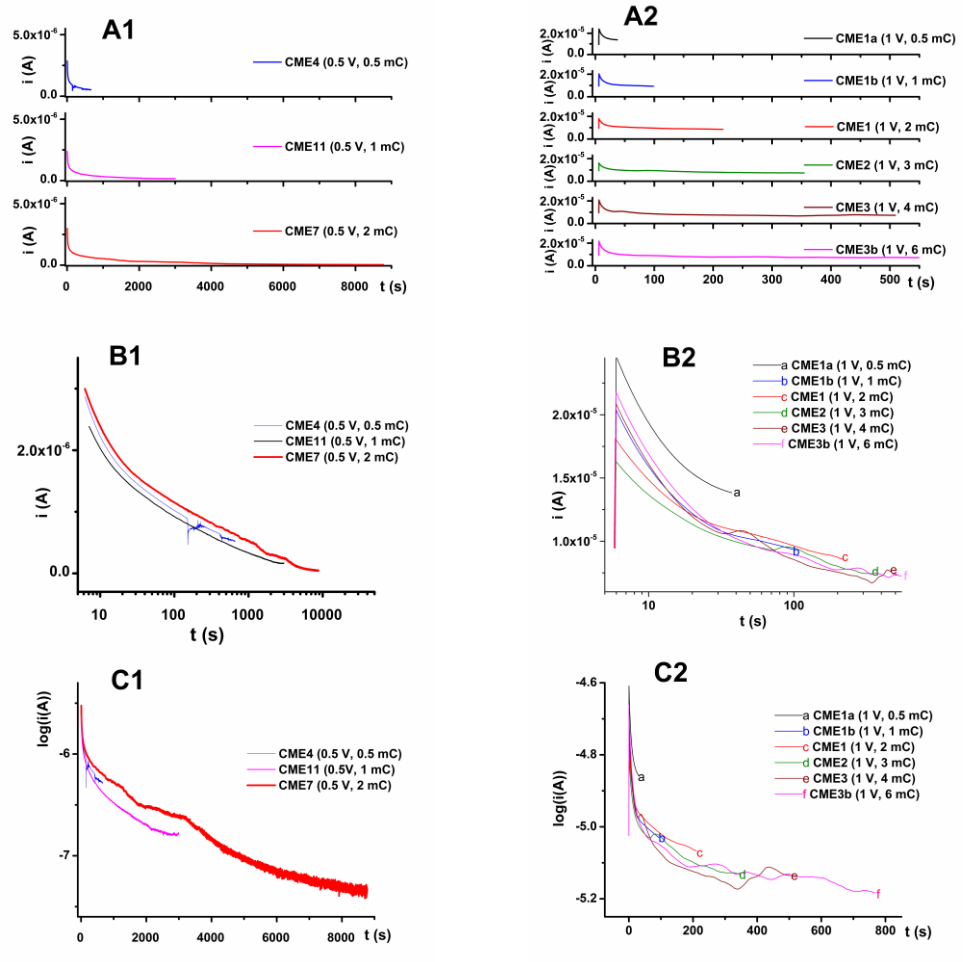

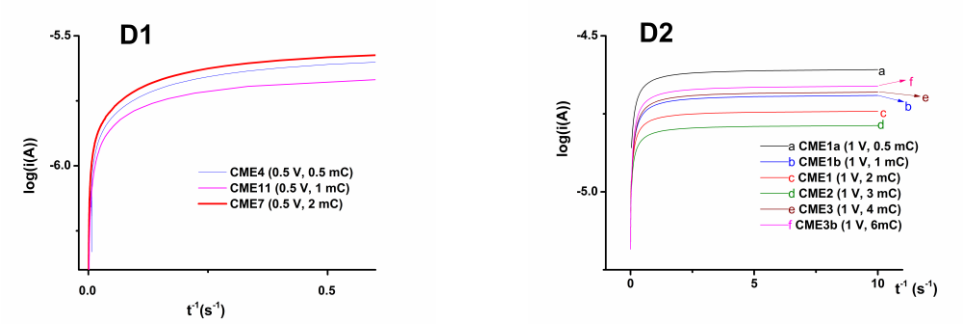

Fig. 4. Chronoamperograms at 0.5 V (A1, B1, C1, D1) and at 1 V (A2, B2, C2, D2) in various coordinates: linear *i-t* (A1, A2); logarithmic *i-t* (B1, B2); *logi-t* (C1, C2) and *logi-t*$^{-1}$ (D1, D2) recorded on GC of 3 mm in diameter; the films were obtained using charges of: 0.5 mC, 1 mC, 2 mC, 3 mC, 4 mC, 6 mC.

Regular curves were obtained for different applied potentials in CPEs, as seen in Figs. 2-4. No linear correlations of *logi-t*$^{-1}$ have been seen in Fig. 2**B**, and in its detail (Fig. 2**C**), or in Fig. 3B. When the applied potential increases the limiting current values of the chronoamperograms are increasing, and the time to reach a constant charge is decreasing, consequently.

Regular chronoamperograms were recorded at each constant potential of 0.5 V (Fig. 4A1 and Fig. 4B1) or 1 V (4A2, Fig. 5A and Fig. 5B), and various charges. Their superposition in different coordinates (Fig. 4B1 and Fig. 4B2, Fig. 4C1 and Fig. 4C2, Fig. 4D1 and Fig. 4D2) indicated a good reproducibility of obtaining **L**-CMEs. The estimated error was of about 5%.

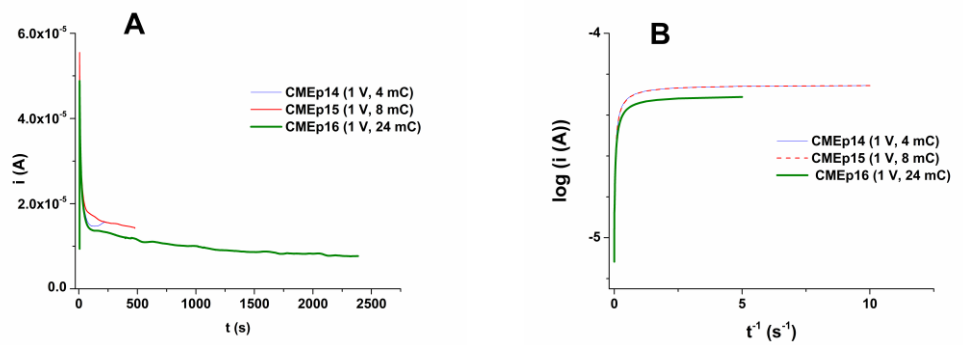

Fig. 5. Chronoamperograms at 1 V in coordinates: *i - t* (A) and *logi - t*$^{-1}$ (B), recorded on GC pellet (6 mm in diameter); the films were obtained using different charges: 4 mC (CMEp14), 8 mC (CMEp15), 24 mC (CMEp16)

Highlighting films formation on L-CMEs in organic electrolytes

For the films' formation evaluation, **L**-CMEs electrodes prepared through CPE on standard GC disks (d = 3 mm) were transferred in TBAP 0.1 M /CH_3CN or in ferrocene solution in TBAP 0.1 M/CH_3CN, and their CV curves were

recorded and compared with those obtained on the bare electrode. The CV curves (Fig 6) obtained in the transfer solution (which contains the supporting electrolyte 0.1 M TBAP/ CH_3CN) on **L**-CMEs showed higher hysteresis than those on bare electrode, both for electrodes prepared by CPE (bold solid line), and by scanning the potential. The presence of the deposited film can be put in evidence also by the appearance of an anodic shoulder at about 0 V and a cathodic peak at about -0.1 V. These potentials are also found for the films prepared by scanning the potential, such as that shown in Fig. 6, for which the CV curve is represented by a solid red line.

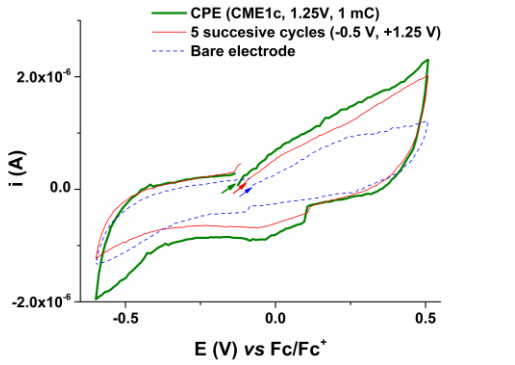

Fig 6. CV curves (50 mV/s) in the supporting electrolyte (0.1 M TBAP/ CH_3CN) on the **L**-CMEs obtained (in 1mM solution of **L** in 0.1 M TBAP/ CH_3CN) by CPE at 1.25V, 1mC on CME1c (solid bold green line), and by 5 successive cycles (50 mV/s) between -0.5V and +1.25V (solid red line), and on the uncovered electrode (dashed blue line)

The transfer of **L**-CMEs into the ferrocene (1 mM) solution in the supporting electrolyte (0.1 M TBAP/ CH_3CN) lead to modified ferrocene curves compared to those obtained on the bare electrode (Fig.7 and Fig.8).

In Fig. 7A and 7B is shown the influence of CPE preparation potential on the chronoamperometric curves obtained in the preparation solution, and on the CV curves in ferrocene transfer solution, respectively. The time to reach 2mC for the applied potential of 0.5 V is about 8800 s. The transfer of this **L**-CME in ferrocene solution shows a CV curve very modified for the ferrocene signal. For **L**-CME prepared at 0.8 V and 2 mC this time is 280 s. The last one has in the transfer solution a signal for ferrocene very close to that for the bare electrode (Fig. 7B). The shape of these CV curves can be explained by looking at the chronoamperograms in Fig. 7A. At the potential of 0.5 V the currents are small, and the polymerization is slow, but there is time enough to deposit the polymer on the electrode; at 0.8 V the currents are high, but there is 31 times less time for film deposition (8800/ 280 ~ 31). For the **L**-CME prepared at 0.8 V, the transfer in ferrocene solution leads to small changes in comparison with the bare electrode: the formal potential of ferrocene (Ef = (Epa+ Epc)/2) is slightly shifted, and the potential shift between the anodic peak and the cathodic peak (ΔEp = Epa - Epc)

increases slightly (Table 2). There are two ways to explain this behavior: a) the films prepared at 0.8 V are very thin/porous in this case, much thinner/porous than those prepared at 0.5 V; b) the films have a different structure/adhesion (the film formed at 0.5 V covers the electrode better, leading to a strong diminution in currents for ferrocene). Compared to the bare electrode, the ferrocene signal on the **L**-CMEs electrodes prepared at 0.8 V and 1 V and transferred into the ferrocene solution exhibits CV curves that depend very little on the synthesis potential and on the charge used for synthesis (Fig. 7B and Fig. 8B, respectively, Table 3). This experiment, also called the "ferrocene redox probe", indicates the porosity of the formed film. If the ferrocene signal is not altered as a peak intensity value or as a peak potential on the **L**-CME relatively to the bare electrode, the film is porous, otherwise it is compact.

Table 2

CV parameters for Fc/Fc^+ on GC and L-CMEs obtained by CPE (2mC) at different potentials (E)

Electrode	E_{pa}	i_{pa}	E_{pc}	i_{pc}	ΔEp	Ef
	(V)	(A)	(V)	(A)	(mV)	(mV)
GC	0.142	9.13E-05	0.020	-4.05E-05	162.0	81.0
L-CME, E = 0.5 V	0.257	6.82E-06	-0.031	-1.47E-06	227.0	113.0
L-CME, E = 0.8 V	0.142	9.09E-05	0.021	-4.24E-05	163.0	82.0

Table 3

CV parameters for Fc/Fc^+ on GC and L-CMEs obtained by CPE (1 V) at different charges (q)

Electrode	E_{pa}	i_{pa}	E_{pc}	i_{pc}	ΔEp	Ef
	(V)	(A)	(V)	(A)	(mV)	(mV)
GC	0.141	5.878E-05	0.030	-3.398E-05	170.0	85.0
L-CME, q = 1 mC	0.135	5.889E-05	0.030	-3.500E-05	165.0	82.0
L-CME, q = 2 mC	0.139	5.889E-05	0.031	-3.540E-05	169.0	85.0
L-CME, q = 3 mC	0.143	5.906E-05	0.031	-3.499E-05	175.0	87.0
L-CME, q = 4 mC	0.140	5.917E-05	0.030	-3.499E-05	170.0	85.0
L-CME, q = 6 mC	0.143	6.000E-05	0.031	-3.499E-05	174.0	87.0

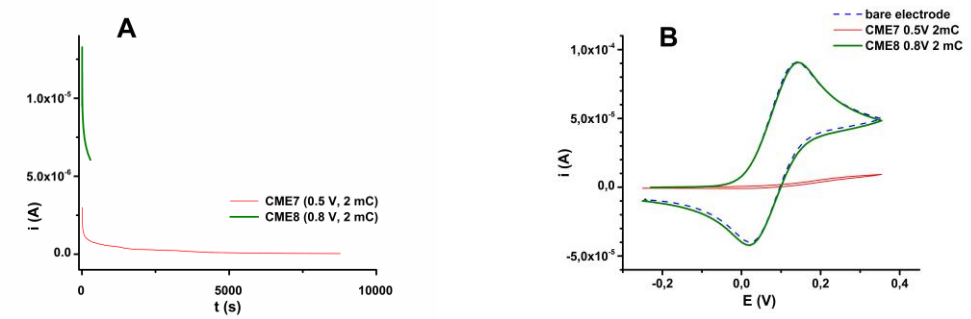

Fig. 7. (**A**) Chronoamperograms in coordinates: *i* - *t* during the preparation of **L**-CMEs, and (**B**) the corresponding CV curves of the transfered CMEs in ferrocene solution in 0.1 M TBAP/ CH_3CN compared to those recorded on the bare electrode (dashed blue line); **L**-CMEs were prepared at different potentials (using the same charge of 2 mC): 0.5 V (CME7 - red, 8800 s), 0.8V (CME8 - green, 280 s)

In Fig. 8, it can be observed that, as the charge used in electropolymerization (1, 2, 3, 4, 6 mC) increases at a constant potential (1 V), the intensity of the ferrocene signal does not change significantly. The ferrocene/ ferricenium system has a similar value of about 100 mV for ΔEp on the CMEs and on the uncovered electrode, which suggests the formation of thin/porous films.

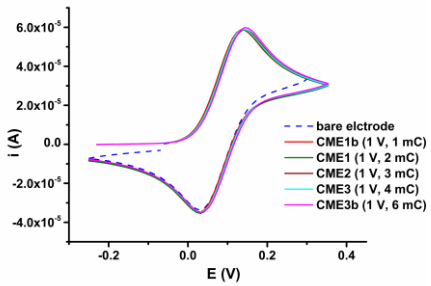

Fig 8. CV curves of the transfered **L**-CME**s** in ferrocene solution in 0.1 M TBAP/ CH_3CN compared to those recorded on the uncovered electrode (dotted line); **L**-CMEs were prepared at 1 V using different charges (Fig. 4**B2**).

Cd, Pb, Cu, Hg analysis using L-CMEs

The complexing properties of **L**-CMEs were investigated using the chemical preconcentration - anodic stripping method, and the influence of different parameters (preparation potential and charge density in CPE) was studied to improve **L**-CMEs performance in the analysis of HMs. During their preparation on standard GC (d = 3 mm) the chronoamperograms were recorded (Fig. 4) to check the charge and reproducibility of synthesis. The dissolution peaks for Cd(II), Pb(II), Cu(II) and Hg(II) are located at about -0.8 V, - 0.55 V, - 0.10 V and + 0.25 V, respectively (vs. Ag| AgCl), as it will be shown further.

Fig. 9A shows the DPV curves obtained for **L**-CMEs which were prepared by CPE at different potentials on GC disks (3 mm in diameter) for a charge of 0.5 mC. The DPV curves for the CME prepared at 0.5 V show distinct signals only for Pb and Cd, having a Δi_{peak} ratio of 6/1; a ratio of 5/1 was obtained for the corresponding films prepared at 1 V (Fig. 9B). The peak areas can be used as an alternative to evaluate the responses to the two cations. The areas ratios for the same peaks for Pb and Cd at 0.5 V and 1 V are 7.7 and 15, respectively. These values reflect the selectivity of **L**-CMEs for Pb.

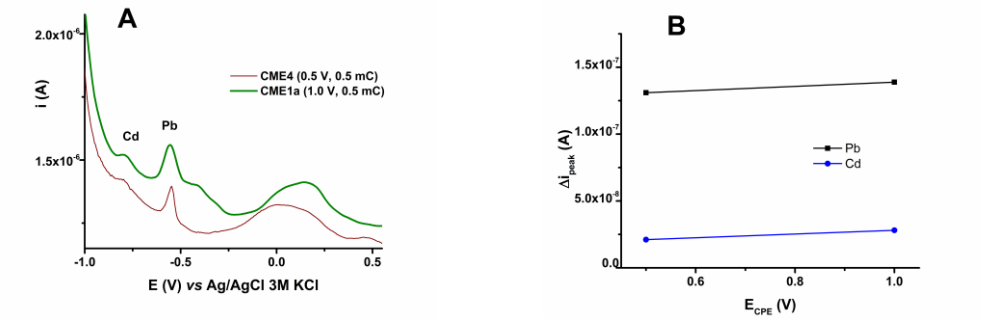

Fig. 9. DPV curves for conditioned **L**-CMEs introduced for 15 minutes in accumulation solution of 10^{-6} M of each HMs (after 3 minutes of polarization at -1 V) – A, and dependence of DPV peak currents (Δi_{peak}) on CPE preparation potential - B; **L**-CMEs were prepared using the same charge of 0.5 mC, but at different potentials (0.5 V and 1 V)

Fig. 10 and 11 show the DPV curves for **L**-CMEs introduced in mixed accumulation solutions of 10^{-6} M and 10^{-5} M of each investigated cations.

Figures 10A and 10B give the DPV curves for the films prepared at 0.5 V and 1.79 mC (corresponding to 26 mC/ cm^2), respectively, the dependencies of the peak DPV currents on the electric charge used in the CPE. A linear increase in peak DPV currents is observed for Pb ($\Delta i_{peak\ Pb}$) with electric charge (Fig. 10B) with a slope of $4.66 \cdot 10^{-7}$ A/ mC. The same linear dependence was noticed also for the surface area of Pb peak ($\Delta A_{peak\ Pb}$) calculated from the DPV curves obtained on CME11. This also proves that the film is porous because the linear dependence shows that cations can penetrate in the films similarly no matter their thickness. A thicker film gives a better signal, which is a very good feature of the film from analytical point of view. Their chronoamperograms as well as the corresponding CV curves in ferrocene transfer solution indicate the fact that reproducible films were formed.

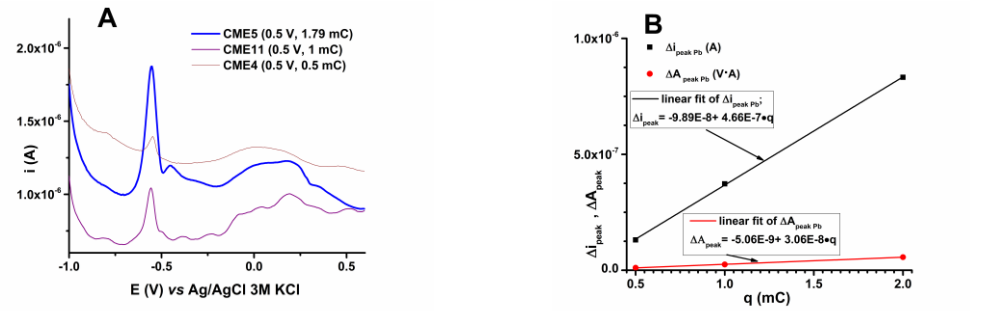

Fig. 10. DPV curves for conditioned **L**-CMEs introduced in accumulation solutions of 10^{-6} M of each HM ion (**A**), and dependence of DPV peak current (Δi_{peak}) and area ($A_{i\ peak\ Pb}$) on charge q used in CPE (**B**); **L**-CMEs were prepared at 0.5 V using different charges: 0.5 mC (thin brown line), 1 mC (purple line), 1.79 mC (bold blue line).

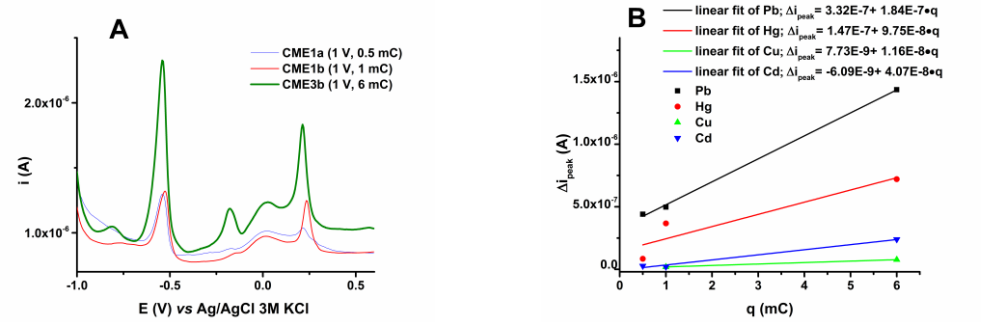

Fig. 11. DPV curves for conditioned **L**-CMEs introduced in accumulation solutions of 10^{-5} M of all HMs (**A**), and dependence of DPV peak currents (Δi_{peak}) on charge q used in CPE (**B**); **L**-CMEs were prepared at **1 V** using different charges: 0.5 mC (thin blue line), 1 mC (red), 6 mC (bold olive line).

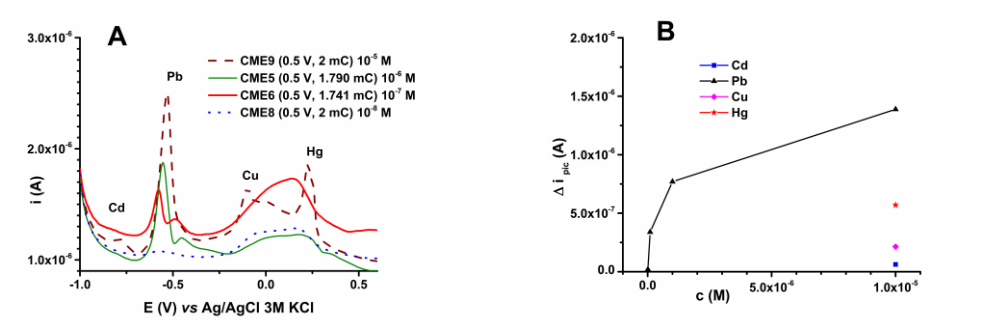

Fig. 12. DPV curves recorded for **L**-CMEs after immersion in HMs mixed solutions of different concentrations *c* (M); 10^{-5} - dash wine line (CME9), 10^{-6} - solid olive line (CME5), 10^{-7} - bold solid red line (CME6), 10^{-8} - dot blue line (CME10); **L**-CMEs were prepared by CPE at 0.5 V and 2 mC in **L** solution (1 mM) in 0.1 M TBAP, CH_3CN.

Fig. 11 confirms the influence of electric charge on the analytical signals of all ions in the synthesis performed by CPE at 1 V and 84 mC/ cm^2. An increase

in charge leads to an increase in analytical signals for all ions, with slopes of $0.4 \cdot 10^{-7}$ (Cd), $1.84 \cdot 10^{-7}$ (Pb), $0.116 \cdot 10^{-7}$ (Cu) and $0.98 \cdot 10^{-7}$ (Hg). It is observed that the slope obtained for Pb at 1 V is lower than that obtained at 0.5 V, although the film is thicker. This shows that the analytical optimal synthesis potential is 0.5 V. Increasing the film thickness leads to signal intensification.

In Fig. 12 is given the calibration curve for HMs analysis build for **L**-CMEs prepared by CPE at 0.5 V and 2 mC in L solution (1 mM).

From Fig. 12A it results that for all metal cations in the solution of 10^{-5} M (for each cation), DPV responses can be noticed, but with different intensities. The highest analytical signals is recorded for Pb(II), followed by Hg(II). At smaller HMs concentrations (10^{-6} M, 10^{-7} M, and 10^{-8} M) **L**-CMEs show a better signal in DPV for Pb(II), which indicates a higher sensitivity for this cation compared to the other cations present in accumulation solutions.

Fig. 12B shows that the signal for Pb(II) increases linearly in the concentration range between 10^{-8} and 10^{-7} M. At higher concentrations the signal attains a limiting value indicating a saturation starting at 10^{-6} M. At this concentration the ratios of the signals for Pb(II)/ Hg(II)/Cu(II)/Cd(II) are of about 19/8/4/1. These ratios underline the selectivity of **L**-CMEs vs Pb(II) analysis.

Surface studies for L-CMEs through SEM and AFM

The complexing properties of **L**-CMEs were also due to the surface characteristics parameters, as seen in previous studies on similar ligands [10, 11]. The influence of preparation potential and charge density in CPE was studied to understand and improve **L**-CMEs performance in the analysis of HMs. The **L**-CMEs with best results in HMs analysis were prepared on bigger GC pellets (d = 6 mm) electrodes (CME12p - CME19p), and their surface was examined by SEM and AFM. During their preparation in 1 mM solutions of **L** in 0.1M TBAP/ CH_3CN by CPE at different charges and potentials the chronoamperograms were also recorded (as previously shown in Figures 2, 3, 5) to check the charge and reproducibility of films preparation.

The morphology of poly**L** films deposited on the surface is given by the SEM and AFM images which allow establishing the characteristics of poly**L** films (Tables 4 - 7).

The images from Table 4 shows that for charge density of 14 mC/ cm^2 there are films at all studied potentials, but they are very thin.

The pictures from Table 5 shows the influence of preparation potential for thicker films prepared with a charge density of 28 mC/ cm^2. Columnar formations confirmed also by AFM (see further) can be noticed at this charge density, and their dimensions were calculated and plotted on the screen when they are more prominent (for the CME17p prepared at 0.5 V). With the increase of potential the formations are less prominent. These SEM images are in agreement with the

chronoamperograms from Fig. 2A. The thickest film which has the longest polymerization time corresponds to the biggest formations seen by SEM.

Table 6 shows the presence of formations are increasingly prominent as the polymerization charge increases; the largest formations are seen in the thickest film (CME 16p), which corresponds to the biggest electropolymerization charge used (84 mC/ cm^2). The results are in agreement with the data from Fig. 11 which show the highest analytical performances for the thickest film obtained at 0.5 V.

Table 4

SEM micrographs at ×100 K for films obtained for 14 mC/cm^2 at different potentials

1 V (CME14p)	**1.5 V** (CME13p)	**2.5 V** (CME12p)
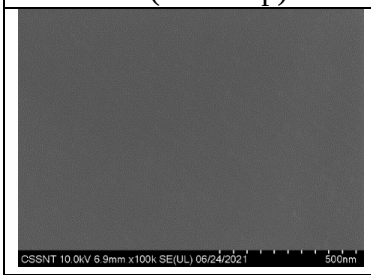	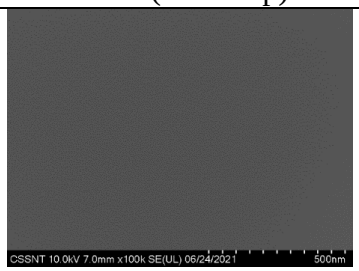	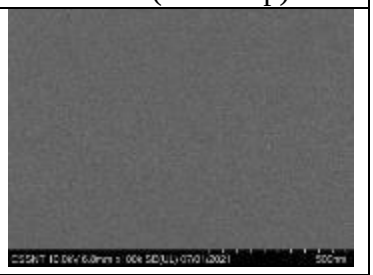

Table 5

EM micrographs at ×100 K for films obtained for 28 mC/cm^2 at different potentials

0.5 V (CME17p)	**0.8 V** (CME19p)	**1 V** (CME15p)
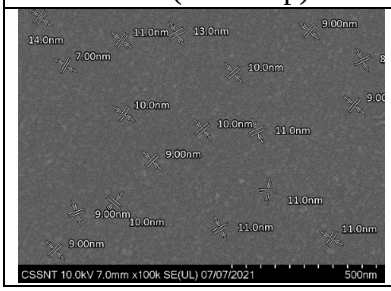	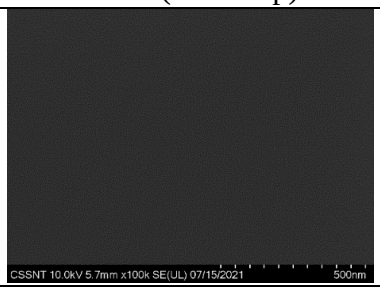	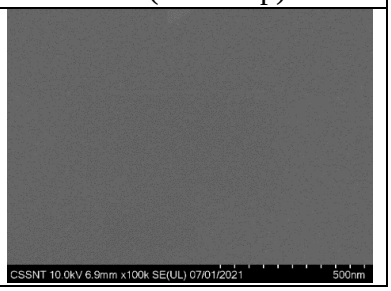

Table 6

SEM micrographs at ×100 K for films obtained at 1V with different polymerization charge densities

14 mC/cm^2 (CME14p)	**28 mC/cm^2** (CME15p)	**84 mC/cm^2** (CME16p)
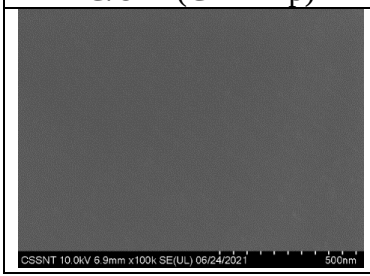	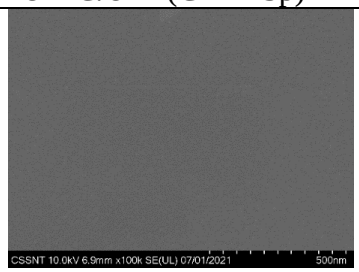	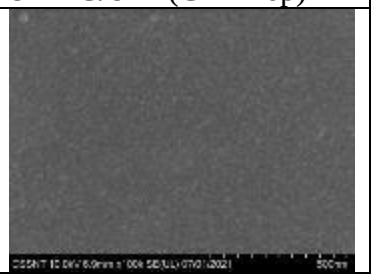

The parameters of the polymer films established by parallel SEM and AFM experiments are presented in Table 7. The surface roughness (RMS), deduced from AFM in a similar way as for other azulene ligands [12], is given in Table 8. The parameters of the square average roughness (RMS) and the average roughness (Ra) of the poly**L** films were calculated from the topographic images generated by the processing software, using the same equations as those applied in case of other azulene derivatives [12]. The columns structures observed in the SEM micrograph for the **L**-CME sample prepared at 0.5 V and 26 mC/ cm^2, were also identified in the AFM measurements. Those columnar structures have a maximum hight of ~ 0.18 µm. The presence of these columns strongly influences the roughness of the sample.

Table 7

SEM micrographs at ×100 K and AFM 3D topography images for films obtained by CPE at 0.5 V with different polymerization charges

Electrode	SEM micrographs at ×100 K	AFM image
CME17p (0.5 V; 28 mC/cm^2)	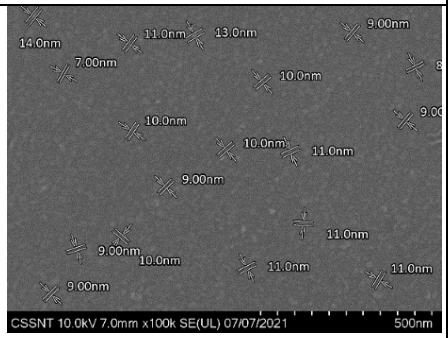	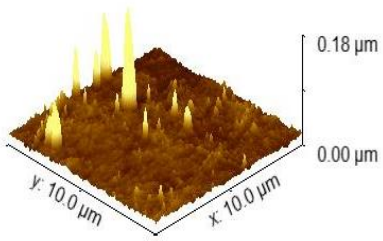
CME18p (0.5V; 26 mC/cm^2)	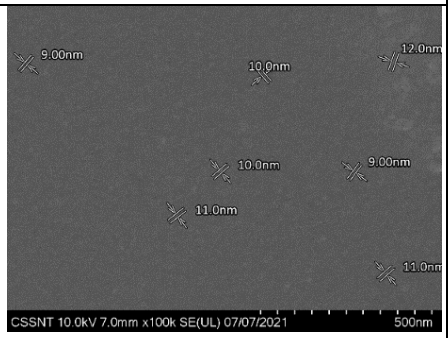	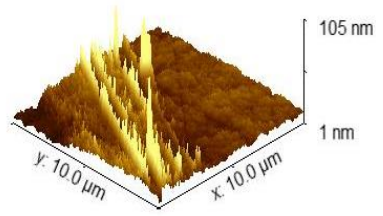

Unmodified electrode	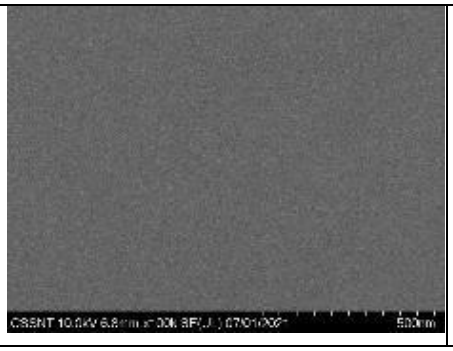	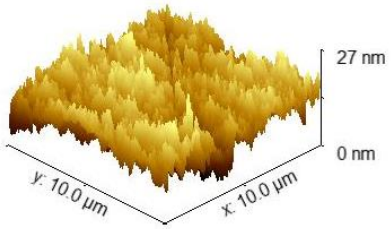

It can be observed that the polymer surface becomes softer and the roughness average (Ra) decreases from 2.57 nm to 2.4 nm when the preparation charge increases from 26 to 28 mC/ cm^2. The film deposition time increases from 5000 s for 26 mC/ cm^2 to about 6000 s for 28 mC/ cm^2. From SEM column results in Table 7 it can be concluded that at 28 mC/ cm^2 the formations are more prominent than at 26 mC/ cm^2, their dimensions being similar: 9-14 nm for 28 mC/ cm^2, and 9-12 nm for 26 mC/ cm^2. From AFM data it results that the maximum height of the columns is about 180 nm at 28 mC/ cm^2, higher than for the film of 26 mC/ cm^2 where the agglomeration of columns with a maximum height of about 105 nm was noticed.

Table 8

Surface roughness values of the samples revealed by the images recorded on 10 µm x 10 µm

Sample	Deposition time	Topography	
	(s)	RMS* (nm)	Ra* (nm)
Bare electrode	-	2.81	2.19
L-CME prepared at 0.5 V and 26 mC/ cm^2	5000	3.38	2.57
L-CME prepared at 0.5 V and 28 mC/ cm^2	6000	4.81	2.40

RMS* - Mean Square Root roughness average; Ra* - Roughness average

Discussions on L-CMEs preparation

During previous research [8] several parameters that influence the HMs analysis when using **L**-CMEs as sensors were varied and their optimal values were established (pH of the acetate buffer solution, open circuit preconcentration time, reduction potential, reduction time). These values were preserved in all experiments performed after. In the present study the optimization on **L**-CMEs aimed to establish the main parameters of the preparation step. Several charge and potential values were tested in order to obtain **L**-CMEs (by CPE in 1 mM **L** solutions in 0.1 M TBAP/ CH_3CN). On GC disks (3mm in diameter) the following tests were done: chronoamperometry, ferrocene redox probe and analysis of HMs (Table 1). In the case of films obtained at the 1 V potential and different electropolymerization charges (1, 2, 3, 4, 6 mC), the deposition time was relatively short (between 100 s and 800 s), and no significant changes of the

ferrocene signal were found compared to the uncovered (bare) electrode. At a potential of 0.5 V (and with a electropolymerization charge of about 2 mC/ 28 mC/cm^2), the deposition time was much longer (of several hours), and the ferrocene signal of the CME in transfer solution was very disrupted compared to the uncovered electrode. At a potential of 0.8 V (and with the same electropolymerization charge density of 28 mC/cm^2), the polymer deposition occurred in an intermediate time (approximately 5 minutes), and the ferrocene signal was only slightly modified compared to that on the uncovered electrode. That is why the polymer films prepared at a potential of 0.5 V and a charge of about 2 mC were used to analyse the cations (Cd^{2+}, Pb^{2+}, Cu^{2+} and Hg^{2+}) in test solutions of different concentrations of HMs.

The morphology of the poly**L** films obtained at different potentials (0.5 V, 0.8 V, 1 V) for a constant electropolymerization charge studied by SEM experiments showed that the polymer film is continuously deposited on the surface of the electrode, presenting columnar formations. Columnar formations confirmed also by AFM were noticed at the potential of 0.5 V. With the increase of potential, the formations are less prominent. The SEM images are in agreement with the chronoamperograms. The thickest film which has the longest polymerization time corresponds to the biggest formations seen by SEM and AFM. The differences appear in AFM results when comparing the average roughness of the polymer film surfaces obtained at different electropolymerization charges (Table 8). The roughness of the polymer is higher when the charge increases.

4. Conclusions

The present study resumes the experiments performed to prepare new chemically modified electrodes based on E-5-((5-isopropyl-3,8-dimethylazulen-1-yl)diazenyl)-1H-tetrazole (L) for heavy metal (HM) ions analysis. CMEs based on L, denoted L-CMEs, were prepared by electropolymerization at different potentials and electrical charge densities. The analytical performances of L-CMEs for the detection of mixed HMs ions in water synthetic solutions were tested. The value of the electropolymerization potential is the main parameter that controls the morphological characteristics of the deposited films. At potentials at the foot of the first oxidation peak for L (0.5 V), porous films are formed which lead to lower detection limits for HMs. Increasing the amount of electropolymerization charge for these films improved the analytical parameters, especially for Pb ion. The main films characteristics (mean square root roughness average, roughness average, columnar formations) were noticed by SEM and AFM. They were connected to other electrochemical features (chronoamperograms during film formation, ferrocene CV peaks potentials in transfer solution, detection current).

Good analytical signals were obtained for all HMs investigated ions in the mixed solution of 10^{-5} M concentration. At lower concentrations (bellow 10^{-7} M), **L**-CMEs have higher sensitivity for Pb(II) than for the other ions.

REFERENCES

[1] *R. Singh, N. Gautam, A. Mishra, R. Gupta*, Heavy metals and living systems: An overview, Indian J. Pharmacol., **vol. 43**, no. 3, 2011, pp. 246-253. doi: 10.4103/0253-7613.81505

[2] *G. S. Shukla, R. L. Singhal*, The present status of biological effects of toxic metals in the environment: lead, cadmium, and manganese, Can J Physiol Pharmacol, **vol. 62**, no. 8, 1984, pp. 1015-1031. doi: 10.1139/y84-171

[3] *P. B. Tchounwou, C. G. Yedjou, A. K. Patlolla, D. J. Sutton*, Heavy Metal Toxicity and the Environment. In: Luch A. (eds) Molecular, Clinical and Environmental Toxicology, Experientia Supplementum, **vol. 101**, Springer, Basel, 2012, pp. 133-164.

[4] *N. H. Bings, A. Bogaerts, J. A. C. Broekaert*, Atomic Spectroscopy: A Review, Anal. Chem., **vol. 82**, no. 12, 2010, pp. 4653-4681.

[5] *G. March, T.D. Nguyen, B. Piro*, Modified Electrodes Used for Electrochemical Detection of Metal Ions in Environmental Analysis. Biosensors. **vol. 5**, 2015, pp. 241–275.

[6] *L. Bîrzan, M. Cristea, V. Tecuceanu, A. Hanganu, E.-M. Ungureanu, A. C. Răzuș*, 5-(Azulen-1-yldiazenyl) tetrazoles; Syntheses and Properties, Rev. Chim., **vol. 71**, no. 5, 2020, pp. 251-264. doi:10.37358/RC.20.5.8133

[7] *A.-M. Păun, O.-T. Matica, V. Anăstăsoaie, L.-B. Enache, E. Diacu, E.-M. Ungureanu*, Recognition of Heavy Metal Ions by Using E-5-((5-Isopropyl-3,8-Dimethylazulen-1-yl)Dyazenyl)-1H-Tetrazole Modified Electrodes, Symmetry, **vol. 13**, no. 4, 2021, pp. 644-654. https://doi.org/10.3390/sym13040644

[8] *A.C. Razus*, Azulene Moiety as Electron Reservoir in Positive Charged Systems; Short Survey., Symmetry, **vol. 13**, 2021, pp. 526, https://doi.org/10.3390

[9] *G.-O. Buică, I.-G. Lazăr, L. Bîrzan, C. Lete, M. Prodana, M. Enăchescu, V. Tecuceanu, A. B. Stoian, E.-M. Ungureanu*, Azulene-ethylenediaminetetraacetic acid: A versatile molecule for colorimetric and electrochemical sensors for metal ions, Electrochim. Acta, **vol. 263**, 2018, pp. 382-390. doi:10.1016/j.electacta.2018.01.059

[10] *M. D. Pop, O. Brîncoveanu, M. Cristea, G.-O. Buică, M. Enăchescu, E.-M. Ungureanu*, AFM and SEM Characterization of Chemically Modified Electrodes Based on 5-[(azulen-1-yl) methylene]-2-thioxothiazolidin-4-one, Rev. Chim., **vol. 68**, no. 12, 2018, pp. 2799-2803. doi:10.37358/rc.17.12.5981

[11] *L.-B. Enache, V. Anăstăsoaie, L. Bîrzan, E.-M. Ungureanu, P. Diao, M. Enăchescu*, Polyazulene-Based Materials for Heavy Metal Ion Detection. 2. (E)-5-(azulen-1-yldiazenyl)-1H-Tetrazole-Modified Electrodes for Heavy Metal Sensing, Coatings, **vol. 10**, no. 9, 2020, pp. 869-883. doi:10.3390/coatings10090869

[12] *V. Anăstăsoaie, C. Omocea, L-B. Enache, L. Anicăi, E-M. Ungureanu, JF. van Staden, M. Enăchescu,* Surface Characterization of New Azulene-Based CMEs for Sensing. Symmetry. **vol. 13**, 2021. https://doi.org/10.3390/sym13122292